

Warm Modified Chaplygin Gas Shaft Inflation

Abdul Jawad^{*}, Amara Ilyas[†] and Shamaila Rani[‡]
 Department of Mathematics, COMSATS Institute of
 Information Technology, Lahore-54000, Pakistan.

Abstract

In this paper, we examine the possible realization of a new family of inflation called “shaft inflation” by assuming the modified Chaplygin gas model and tachyon scalar field. We also consider the special form of dissipative coefficient as $\Gamma = a_0 \frac{T^3}{\phi^2}$ and calculate the various inflationary parameters in the scenario of strong and weak dissipative regimes. In order to examine the behavior of inflationary parameters, the planes of $n_s - \phi$, $n_s - r$ and $n_s - \alpha_s$ (where n_s , α_s , r and ϕ represent spectral index, its running, tensor to scalar ratio and scalar field respectively) are being developed which lead to the constraints: $r < 0.11$, $n_s = 0.96 \pm 0.025$ and $\alpha_s = -0.019 \pm 0.025$. It is quite interesting that these results of inflationary parameters are compatible with BICEP2, WMAP (7 + 9) and recent Planck data.

Keywords: Inflationary Cosmology; Tachyon field model; Modified Chaplygin Gas; Shaft potential; Inflationary Parameters.

PACS: 05.40.+j; 98.80.

1 Introduction

Inflation is the most acceptable paradigm that describes the physics of the very early universe. Besides of solving most of the shortcomings of the hot

^{*}jawadab181@yahoo.com; abduljawad@ciitlahore.edu.pk

[†]amara_ilyas14@yahoo.com

[‡]shamailator.math@yahoo.com, drshamailarani@ciitlahore.edu.pk

big-bang scenario, like the horizon, the flatness and the monopole problems [1]-[6], inflation also generates a mechanism to explain the large-scale structure (LSS) of the universe [7]-[11] and the origin of the anisotropies observed in the cosmic microwave background (CMB) radiation [12]-[19]. The primordial density perturbations may be sourced from quantum fluctuations of the inflaton scalar field during the inflationary expansion. The standard cold inflation scenario is divided into two regimes: the slow-roll and reheating phases. In the slow-roll period, the universe undergoes an accelerated expansion and all interactions between the inflaton scalar field and other field's degrees of freedom are typically neglected. Subsequently, a reheating period [20, 21] is invoked to end the brief acceleration. After reheating, the universe is filled with relativistic particles and thus the universe enters in the radiation big-bang epoch. For a modern review of reheating, see [22].

On the other hand, warm inflation is an alternative mechanism for having successful inflation. The warm inflation scenario, as opposed to standard cold inflation, has the essential feature that a reheating phase is avoided at the end of the accelerated expansion due to the decay of the inflaton into radiation and particles during the slow-roll phase [23, 24]. During warm inflation, the temperature of the universe did not drop dramatically and the universe can smoothly entered into the decelerated, radiation-dominated period, which is essential for a successful big-bang nucleosynthesis. In the warm inflation scenario, dissipative effects are important during the accelerated expansion, so that radiation production occurs concurrently with the accelerated expansion. The dissipative effect arises from a friction term Γ which describes the processes of the scalar field dissipating into a thermal bath via its interaction with other field's degrees of freedom.

The effectiveness of warm inflation may be parameterized by the ratio $R \equiv \Gamma/3H$. The weak dissipative regime for warm inflation is for $R \ll 1$, while for $R \gg 1$, it is the strong dissipative regime. Following Refs.[25, 26], a general parametrization of the dissipative coefficient depending on both the temperature of the thermal bath T and the inflaton scalar field ϕ can be written as

$$\Gamma(T, \phi) = C_\phi \frac{T^m}{\phi^{m-1}}, \quad (1)$$

where the parameter C_ϕ is related with the dissipative microscopic dynamics, the exponent m is an integer whose value is depends on the specifics of the model construction for warm inflation and on the temperature regime of the thermal bath. Typically, it is found that $m = 3$ (low temperature), $m = 1$

(high temperature) or $m = 0$ (constant dissipation).

Later on, Linde [27] introduced the chaotic inflation by realizing that the initial conditions for scalar field driving inflation which may help in solving the persisting inflationary problems. A plethora of works in the subject of warm inflation along with chaotic potential have been done. For instance, Herrera [28] investigated the warm inflation in the presence of chaotic potential in loop quantum cosmology and found consistencies of results with observational data. Del campo and Herrera [29] discussed the warm inflationary model in the presence of standard scalar field, dissipation coefficient of the form $\Gamma \propto \phi^n$ and generalized Chaplygin gas (GCG) and extract various inflationary parameters. Setare and Kamali investigated warm tachyon inflation by assuming intermediate [30] and logamediate scenarios [31]. Bastero-Gill et al. [32] obtained the expressions for the dissipation coefficient in supersymmetric (SUSY) models and their result provides possibilities for realization of warm inflation in SUSY field theories. Bastero-Gill et al. [33] have also explored inflation by assuming the quartic potential. Herrera et al. [34] studied intermediate inflation in the context of GCG using standard and tachyon scalar field.

Panotopoulos and Vidaela [35] discussed the warm inflation by assuming quartic potential and decay rate proportional to temperature and found that the results of inflationary parameters are compatible with the latest Planck data. Moreover, many authors have investigated the warm inflation in various alternative as well as modified theories of gravity [36, 37]. Recently, a new family of inflation models is being developed named as shaft inflation [38]. The idea of this inflation was that the inflationary flatness is effected by shaft i.e; when the scalar field found itself nearest to one of them, it slow-rolls inside the shaft, until inflation ends and gives way to the hot big bang cosmology. The generalized form of shaft potential is

$$V(\phi) = \frac{M_p^4 \phi^{2n-2}}{(\phi^n + m^n)^{2-\frac{2}{n}}}, \quad (2)$$

where M_p, m, n are massless constants.

In the present, we discuss the warm inflation by assuming shaft potential, modified Chaplygin gas model and tachyon scalar field. We will extract the inflationary parameters. The formate of the paper is as follows: In the next section, we will discuss the detailed inflationary scenario with tachyon field and generalized dissipative coefficient. Section **3** and **4** contains the

information about disordered parameters for shaft potential in strong and weak dissipative regimes, respectively. In section 5, the results are given in summarized form.

2 Tachyon Scalar Field Inflationary Scenario

The universe undergoes an accelerated expansion of the universe. The responsible for this acceleration of the late expansion is an exotic component having a negative pressure, usually known as dark energy (DE). Several models have been already proposed to be DE candidates, such as cosmological constant [39], quintessence [40]-[42], k-essence [43]-[45], tachyon [46]-[48], phantom [49]-[51], Chaplygin gas [52], holographic dark energy [53], among others in order to modify the matter sector of the gravitational action. Despite the plenty of models, the nature of the dark sector of the universe, i.e. DE and dark matter, is still unknown. There exists another way of understanding the observed universe in which dark matter and DE are described by a single unified component. Particularly, the Chaplygin gas [52] achieves the unification of DE and dark matter. In this sense, the Chaplygin gas behaves as a pressureless matter at the early times and like a cosmological constant at late times. The original Chaplygin gas is characterized by an exotic equation of state with negative pressure

$$p = -\frac{\beta}{\rho}, \quad (3)$$

with β being a constant parameter. The original Chaplygin gas has been extended to the so-called generalized Chaplygin gas (GCG) with the following equation of state [54]

$$p_{gcg} = -\frac{\beta}{\rho^\sigma}, \quad (4)$$

with $0 \leq \sigma \leq 1$. For the particular case $\lambda = 1$, the original Chaplygin gas is recovered. The main motivation for studying this kind of model comes from string theory. The Chaplygin gas emerges as an effective fluid associated with D-branes which may be obtained from the Born-Infeld action [55]. At background level, the GCG is able to describe the cosmological dynamics [56], however the model presents serious issues at perturbative level [57]. Thus, a modification to the GCG, results in the modified Chaplygin gas (MCG) with

an equation of state given by [58]

$$p = \omega\rho - \frac{\beta}{\rho^\sigma}, \quad (5)$$

where ω is a constant parameters with $0 \leq \sigma \leq 1$, is suitable to describe the evolution of the universe [59, 60] which is also consistent with perturbative study [61].

The energy conservation equation for MCG model turns out to be

$$\rho_{mcg} = \left(\frac{\beta}{1+\omega} + \frac{v}{a^{3(1+\sigma)(1+\omega)}} \right)^{\frac{1}{1+\sigma}}, \quad (6)$$

where v is constant of integration. In spatially flat FRW model, Friedmann equation described as

$$H^2 = \frac{1}{3M_p^2}(\rho_m + \rho_\gamma), \quad (7)$$

where ρ_m is the energy density of matter field and ρ_γ is the energy density of radiation field. The warm MCG model modifies first Friedmann equation which has been used in Eq.(7) reduces to

$$H^2 = \frac{1}{3M_p^2} \left[\left(\frac{\beta}{1+\omega} + v\rho_\phi^{(1+\sigma)(1+\omega)} \right)^{\frac{1}{1+\sigma}} + \rho_\gamma \right], \quad (8)$$

which is named as Chaplygin gas inspired inflation. The energy density and pressure of tachyon scalar field are defined as follows [62],

$$\rho_\phi = \frac{V(\phi)}{\sqrt{1-\dot{\phi}^2}}, \quad p_\phi = -V(\phi)\sqrt{1-\dot{\phi}^2}. \quad (9)$$

The inflaton and imperfect fluid energy densities according to the Eq. (9) are conserved as

$$\dot{\rho}_\phi + 3H(\rho_\phi + p_\phi) = -\Gamma\dot{\phi}^2, \quad (10)$$

$$\dot{\rho}_\gamma + 4H\rho_\gamma = \Gamma\dot{\phi}^2, \quad (11)$$

where Γ is the dissipation factor that evaluates the rate of decay of ρ_ϕ into ρ_γ . It is also important to note that this decay rate can be used as a function

of the temperature of the thermal bath and the scalar field, i.e., $\Gamma(T, \phi)$ or a function of only temperature of thermal bath $\Gamma(T)$, or a function of scalar field only $\Gamma(\phi)$, or simply a constant.

The second law of thermodynamics indicates that Γ must be positive, so the inflaton energy density decompose into radiation density. The second conservation equation is given by

$$\begin{aligned} \frac{\ddot{\phi}}{1 - \dot{\phi}^2} + 3H\dot{\phi} + \frac{V'(\phi)}{V(\phi)} &= -\frac{\Gamma\dot{\phi}}{V}\sqrt{1 - \dot{\phi}^2}, \\ \Rightarrow \ddot{\phi} + \left(3H + \frac{\Gamma}{V}\right)\dot{\phi} &= -\frac{V'(\phi)}{V(\phi)}, \quad \dot{\phi} \ll 1 \\ \Rightarrow 3H(1 + R)\dot{\phi} &= -\frac{V'(\phi)}{V(\phi)}, \quad \text{where } \ddot{\phi} \ll \left(3H + \frac{\Gamma}{V}\right)\dot{\phi}, \end{aligned} \quad (12)$$

where $R = \frac{\Gamma}{3HV}$. In weak dissipative epoch, $R \ll 1$ runs to $\Gamma \ll 3H$ while $R \gg 1$ indicates the high dissipative regime. Here, we assume some constraints which leads to static epoch, i.e., $\rho_\phi \approx V(\phi)$, slow-roll limit, $V(\phi) \gg \dot{\phi}^2$, $(3H + \Gamma)\dot{\phi} \gg \ddot{\phi}$, quasi-stable decay of ρ_ϕ into ρ_γ , $4H\rho_\gamma \gg \dot{\rho}_\gamma$ and $\Gamma\dot{\phi}^2 \gg \dot{\rho}_\gamma$. As we know that the energy density of scalar field is much greater than the energy density of radiations but also at the same time, the energy can be larger than the expansion rate with $\rho_\gamma^{\frac{1}{4}} > H$. This is approximately equal to $T > H$ by considering thermalization, which is true condition to take place in warm inflation. With the help of all these limits Eqs. (7), (11) and (12) become

$$H^2 = \frac{1}{3M_p^2} \left(\frac{\beta}{1 + \omega} + v\rho_\phi^{(1+\sigma)(1+\omega)} \right)^{\frac{1}{1+\sigma}}, \quad (13)$$

$$4H\rho_\gamma = \Gamma\dot{\phi}^2, \quad (14)$$

$$3H(1 + R)\dot{\phi} = -\frac{V'(\phi)}{V(\phi)}, \quad (15)$$

where prime represents the derivative with respect to ϕ .

The energy density of radiation can be used as $C_\gamma T^4$ when we have taken the thermalization. Here $C_\gamma = \pi^2 g_*/30$, where g_* shows the degree of freedom. This expression gives the value as $C_\gamma \simeq 70$ with $g_* = 228.75$. The temperature of thermal bath can be obtained by merging the Eqs. (14) and

(15)

$$T = \left(\frac{\Gamma V'^2}{36C_\gamma H^3 V^2 (1+R)^2} \right)^{\frac{1}{4}}, \quad (16)$$

where $\Gamma = a_0 \frac{T^q}{\phi^{q-1}}$, which is the general form of dissipative coefficient, while a_0 and q are constant parameters associated with dissipative microscopic dynamics. The consequences of radiation are studied during inflation through this kind of dynamic which is suggested first time in warm inflation with theoretical basis of supersymmetry (SUSY) [63, 64].

A set of dimensionless slow-roll parameters must be satisfied for the occurrence of warm inflation which are defined in the form of Hubble parameter as [65]

$$\epsilon = -\frac{\dot{H}}{H^2}, \quad \eta = -\frac{\ddot{H}}{H\dot{H}}.$$

The slow-roll parameters can also be deduced in the form of scalar field and thermalization according to the tachyon field along with modified Chaplygin gas, which are defined as

$$\begin{aligned} \epsilon &= \frac{v(1+\omega)M_p^2 V^{(1+\sigma)(1+\omega)-2} V'^2}{2(1+R) \left(\frac{\beta}{1+\omega} + vV^{(1+\sigma)(1+\omega)} \right)^{1+\frac{1}{1+\sigma}}}, \\ \eta &= \frac{M_p^2}{(1+R) \left(\frac{\beta}{1+\omega} + vV^{(1+\sigma)(1+\omega)} \right)^{\frac{1}{1+\sigma}}} \left[\frac{((1+\sigma)(1+\omega)-2)V'^2}{V^2} + \frac{2V''}{V} \right] \\ &- 2(1+\sigma)\epsilon. \end{aligned}$$

We can describe number of e-folds in terms of Hubble parameter as well as inflaton

$$N(\phi) = \int_{t_i}^{t_f} H dt = \int_{\phi_i}^{\phi_f} \frac{H}{\dot{\phi}} d\phi, \quad (17)$$

where ϕ_i and ϕ_f can be calculated with the help of first and second slow-roll parametric conditions, i.e., $\epsilon = 1+R$ and $|\eta| = 1+R$.

Next, we will calculate some inflationary parameters such as tensor and scalar power spectra (P_R, P_g), tensor and scalar spectral indices (n_R, n_s). The form of scalar power spectrum can be estimated as $P_R(k_0) \equiv \frac{25}{4} \delta_H^2(k_0)$, where density disorders $\delta_H^2(k_0) \equiv \frac{k_F(T_R)}{2\pi^2}$ and $k_F = \sqrt{\Gamma H}$. However, the amplitude of the tensor and scalar power spectrum of the curvature perturbation are

given by

$$P_R \simeq \left(\frac{H}{2\pi}\right)^2 \left(\frac{3H^2}{V'}\right)^2 \left(\frac{T}{H}\right) (1+R)^{\frac{5}{2}}, \quad P_g \simeq 24\kappa \left(\frac{H}{2\pi}\right)^2. \quad (18)$$

The tensor-to-scalar ratio can be computed by using the relation $r = \frac{P_R}{P_g}$. However, the spectral index and running of spectral index are defined as [66]

$$n_s = 1 + \frac{d \ln P_R}{d \ln k}, \quad \alpha_s = \frac{dn_s}{d \ln k}. \quad (19)$$

Here, the interval in wave number k is referred to the number of e-folds N , through the expression as

$$d \ln k = -dN. \quad (20)$$

In the following, we will evaluate the inflationary parameters for weak and strong dissipative regimes.

3 Inflationary Parameters in Strong Epoch with Shaft Potential

The special case of shaft potential where $n = 2$ is considered for which Eq.(2) takes the form as $V(\phi) = \frac{M_p^4 \phi^2}{(\phi^2 + m^2)}$. The temperature of the radiation for present model with the help of shaft potential, Eq. (16) takes the following form

$$T = \left(\frac{m^6 M_p^5 \sqrt{3 \left(\frac{\beta}{1+\omega} + v \left(\frac{M_p^4 \phi^2}{m^2 + \phi^2} \right)^{(1+\omega)(1+\sigma)} \right)^{-\frac{1}{1+\sigma}}}}{a_0 (m^2 + \phi^2)^3 \left(M_p^4 - \frac{M_p^4 \phi^2}{m^2 + \phi^2} \right) C_\gamma} \right)^{\frac{1}{7}}. \quad (21)$$

The number of e-folds can be calculated by Eq. (17) with $\dot{\phi} = \frac{-V'}{3HVR}$ for strong regime as

$$N = \frac{a_0^{\frac{4}{7}}}{23^{2/7} m^{\frac{2}{7}} M_p^{\frac{4}{7}}} \int_{\phi_i}^{\phi_f} \left(\sqrt{\left(\frac{\beta}{1+\omega} + v \left(\frac{M_p^4 \phi^2}{m^2 + \phi^2} \right)^{(1+\omega)(1+\sigma)} \right)^{\frac{1}{1+\sigma}}} \right)^{\frac{10}{7}}$$

$$\times \left(\frac{(m^2 + \phi^2)^{\frac{1}{7}}}{C_\gamma^{3/7} \phi} \right) d\phi. \quad (22)$$

For the strong epoch, ϕ_i and ϕ_f can be described by considering $\epsilon = R$ and $|\eta| = R$ respectively. The power spectrum attains the value from Eq.(18) as follows

$$P_R = \frac{a_0^{10/7} \left(\frac{m^2 M_p^4}{m^2 + \phi^2} \right)^{10/7}}{483^{3/14} \pi^2 C_\gamma^{15/14}} \left(\frac{\left(\frac{\beta}{1+\omega} + v \left(\frac{M_p^4 \phi^2}{g^2 + \phi^2} \right)^{(1+\omega)(1+\sigma)} \right)^{\frac{1}{2(1+\sigma)}}}{M_p} \right)^{10/7} \\ \times \left(\frac{\left(\frac{m^2 M_p^4 \phi}{(m^2 + \phi^2)^2} \right)^{1/7}}{m^{20/7} \left(\frac{M_p^4 \phi^2}{m^2 + \phi^2} \right)^{25/7}} \right).$$

The scalar power spectrum is given by

$$P_g = \frac{2}{9\pi M_p^4} \left(\frac{\beta}{1+\omega} + v V^{(1+\sigma)(1+\omega)} \right)^{\frac{1}{1+\sigma}}. \quad (23)$$

The tensor-to-scalar ratio can be found by using expression (23) which yields

$$r = \frac{32m^2 M_p^5 v \phi \left(\frac{m^2 M_p^4 \phi}{(m^2 + \phi^2)^2} \right)^{15/7} \left(\frac{M_p^4 \phi^2}{m^2 + \phi^2} \right)^{\frac{3}{7} + \omega + \sigma + \omega\sigma} 3^{2/7} (1+\omega) a_0 C_\gamma^{3/7}}{\left(\frac{a_0 m^4 M_p^4}{m^2 + \phi^2} \right)^{11/7} \left(v \left(\frac{M_p^4 \phi^2}{m^2 + \phi^2} \right)^{(1+\sigma)(1+\omega)} + \frac{\beta}{1+\omega} \right)^{1 + \frac{1}{2(1+\sigma)}}} \\ \times \left(\frac{\left(v \left(\frac{M_p^4 \phi^2}{m^2 + \phi^2} \right)^{(1+\sigma)(1+\omega)} + \frac{\beta}{1+\omega} \right)^{\frac{1}{2+2\sigma}}}{M_p} \right)^{3/7}.$$

Figure 1 shows the plot of tensor-to-scalar ratio versus spectral index within strong regime. This ratio is being plotted for three different values of m with the condition $m < \phi$. Red line has been plotted for $m = 0.2$, green dashed line for $m = 0.5$ and blue dotted line for $m = 0.9$. According to the plot, ratio is not satisfied with spectral index when $m = 0.2$ while tensor-to-scalar ratio is compatible with the spectral index for other two values.

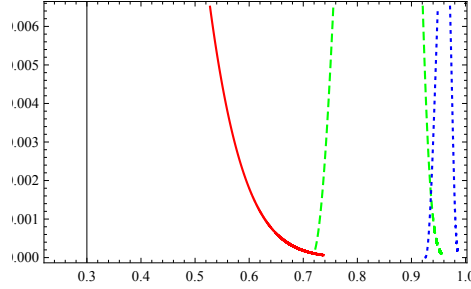


Figure 1: Plot of tensor-to-scalar ratio verses spectral index in strong epoch with $a_0 = 2 \times 10^6$.

However, the spectral index and it's running attained the values by using Eqs. (19) and (20) as

$$n_s = 1 - \left(\frac{23^{2/7} \phi^3 C_\gamma^{3/7} M_p^8 \left(\frac{m^4 a_0 M_p^4}{m^2 + \phi^2} \right)^{3/7}}{7 (m^2 + \phi^2)^5 a_0 \left(\frac{m^2 \phi M_p^4}{(m^2 + \phi^2)^2} \right)^{13/7} \left(\frac{\beta}{1+\omega} + v \left(\frac{\phi^2 M_p^4}{m^2 + \phi^2} \right)^{(1+\sigma)(1+\omega)} \right)} \right) \\ \times \frac{\left(\frac{\beta(49m^2 + 23\phi^2)}{1+\omega} - v(-23\phi^2 + m^2(-39 + 10\omega)) \left(\frac{\phi^2 M_p^4}{m^2 + \phi^2} \right)^{(1+\sigma)(1+\omega)} \right)}{\left(\frac{\phi^2 M_p^3 \left(\frac{\beta}{1+\omega} + v \left(\frac{\phi^2 M_p^4}{m^2 + \phi^2} \right)^{(1+\sigma)(1+\omega)} \right)^{\frac{1}{2+2\sigma}}}{m^2 + \phi^2} \right)^{4/7}}.$$

We plot spectral index n_s versus scalar field ϕ in Figure 2 and notice that red line which represents the behavior of spectral index with respect to ϕ for $m = 0.2$ requires a very large value of ϕ to reach in the range of spectral index. The other two different values i.e., $m = 0.5$ and $m = 0.9$ with green and blue lines respectively, satisfies the range of spectral index for $\phi \in [1, 50]$. It can be observed that the tensor-to-scalar ratio (r) remains less than 0.11 for the range of spectral index $0.96 < n_s < 0.97$ in the strong dissipative epoch.

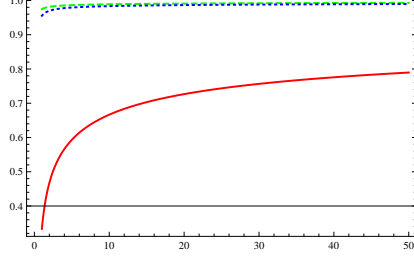


Figure 2: Plot of spectral index number w.r.t inflaton in strong epoch with $a_0 = 2 \times 10^6$.

The running of spectral index becomes

$$\begin{aligned}
\alpha_s = & - \left[83^{4/7} \phi C_\gamma^{6/7} \left(\frac{m^2 \phi M_p^4}{(m^2 + \phi^2)^2} \right)^{9/7} \left(\frac{m^4 a_0 M_p^4}{m^2 + \phi^2} \right)^{6/7} \left(\left(\frac{\beta}{1 + \omega} \right)^2 (231 m^2 \phi^2 \right. \right. \\
& + 23 \phi^4) + 2 \frac{v \beta}{1 + \omega} (23 \phi^4 + m^2 \phi^2 (214 - 17 \omega) + 7 m^4 (1 + \omega) (12 + 5 \omega + 5 \sigma \\
& \times (1 + \omega))) \left(\frac{\phi^2 M_p^4}{m^2 + \phi^2} \right)^{(1 + \sigma)(1 + \omega)} + v^2 (23 \phi^4 + m^2 \phi^2 (197 - 34 \omega) - 2 m^4 \\
& \times (1 + \omega) (-39 + 10 \omega)) \left(\frac{\phi^2 M_p^4}{m^2 + \phi^2} \right)^{2(1 + \sigma)(1 + \omega)} \left. \right] (49 m^{10} a_0^2 M_p^4)^{-1} \left(\frac{\beta}{1 + \omega} \right. \\
& \left. + v \left(\frac{\phi^2 M_p^4}{m^2 + \phi^2} \right)^{(1 + \sigma)(1 + \omega)} \right)^{-2} \left(\frac{\phi^2 M_p^3 \left(\frac{\beta}{1 + \omega} + v \left(\frac{\phi^2 M_p^4}{m^2 + \phi^2} \right)^{(1 + \sigma)(1 + \omega)} \right)^{\frac{1}{2 + 2\sigma}}}{m^2 + \phi^2} \right)^{-8/7} .
\end{aligned}$$

The plot of running of spectral index with respect to scalar field is shown in Figure 3. The suggested values for running of spectral index by WMAP7 [67, 68] and WMAP9 [69] are approximately equal to -0.992 ± 0.019 and -0.019 ± 0.025 , respectively. It can be observed that this parameter is compatible with observational data for $m = 0.5$ and $m = 0.9$. However for $m = 0.2$, the plot of running of spectral index is not compatible with the required range of spectral index.

Figure 3: Plot for running of spectral index versus spectral index in strong epoch with $a_0 = 2 \times 10^6$.

4 Inflationary Parameters in Weak Epoch with Shaft Potential

Here we study the tachyon model in weak epoch ($R \ll 1$), the temperature of the radiation for present model with the help of shaft potential, Eq. (21) takes the form as

$$T = \frac{a_0 m^4 M_p^3 \left(\frac{\beta}{1+\omega} + v \left(\frac{\phi^2 M_p^4}{m^2 + \phi^2} \right)^{(1+\sigma)(1+\omega)} \right)^{-\frac{3}{2(1+\sigma)}}}{\sqrt{3} \phi^4 (m^2 + \phi^2)^2 C_\gamma}. \quad (24)$$

The number of e-folds can be calculated by Eq. (17) with $\dot{\phi} = \frac{-V'}{3HV}$ as

$$N = \frac{1}{2m^2 M_p^2} \int_{\phi_i}^{\phi_f} \left(\frac{\beta}{1+\omega} + v \left(\frac{\phi^2 M_p^4}{m^2 + \phi^2} \right)^{(1+\sigma)(1+\omega)} \right)^{\frac{1}{1+\sigma}} (m^2 + \phi^2) \phi d\phi,$$

where ϕ_i and ϕ_f can be found by taking $\epsilon = 1$ and $|\eta| = 1$ respectively.

The power spectrum attains the value from Eq.(18) as

$$P_r = \frac{(m^2 + \phi^2)^3 a_0}{48m^2 \pi^2 \phi^6 C_\gamma M_p^{14}} \left[M_p^4 - \frac{\phi^2 M_p^4}{m^2 + \phi^2} \right] \left[\frac{\beta}{1+\omega} + v \left(\frac{\phi^2 M_p^4}{m^2 + \phi^2} \right)^{(1+\sigma)(1+\omega)} \right]^{\frac{1}{1+\sigma}}.$$

The scalar power spectrum remains same as for the strong regime. The tensor-to-scalar ratio is obtained by using expressions of power spectrum

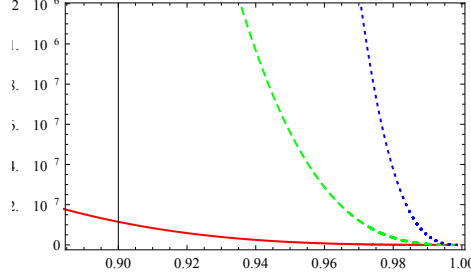


Figure 4: Plot of tensor-to-scalar ratio verses spectral index in weak epoch with $a_0 = 2 \times 10^6$.

and scalar spectrum, which is given by

$$r = \frac{8M_p^2(1+\omega)v}{\left(\frac{M_p^4\phi^2}{m^2+\phi^2}\right)^{2-(1+\omega)(1+\sigma)}} \left(\frac{2M_p^4\phi}{m^2+\phi^2} - \frac{2M_p^4\phi^3}{(m^2+\phi^2)^2} \right)^2 \times \left(\frac{\beta}{1+\omega} + v \left(\frac{M_p^4\phi^2}{m^2+\phi^2} \right)^{(1+\omega)(1+\sigma)} \right)^{-1-\frac{1}{1+\sigma}}.$$

Figure 4 shows the plot of tensor-to-scalar ratio versus spectral index within weak regime. Tensor-to-scalar ratio is being plotted for three different values of m with the condition $m < \phi$. Red line has been plotted for $m = 0.2$, green dashed line for $m = 0.5$ and blue dotted line for $m = 0.9$. According to the plot, there is no change in the behavior of tensor-to-scalar ratio for spectral index while tensor-to-scalar ratio is compatible with the spectral index for all values of m .

The value of spectral index is found with the help of above motioned power spectrum along with first part of Eq.(19) and Eq.(20). It is given as follows

$$n_s = 1 + \left(\frac{\beta}{1+\omega} + v \left(\frac{M_p^4\phi^2}{m^2+\phi^2} \right)^{(1+\omega)(1+\sigma)} \right)^{\frac{-1}{1+\sigma}} \left[\frac{8m^6 M_p^{10}(1+\omega)v\phi}{(m^2+\phi^2)^5} \right] \times \left(\frac{M_p^4\phi^2}{m^2+\phi^2} \right)^{(1+\omega)(1+\sigma)} \left(\frac{\beta}{1+\omega} + v \left(\frac{M_p^4\phi^2}{m^2+\phi^2} \right)^{(1+\omega)(1+\sigma)} \right)^{-1}$$

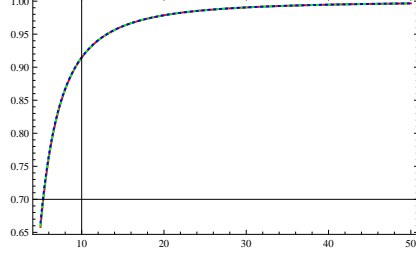


Figure 5: Plot of spectral index number w.r.t inflaton in weak epoch with $a_0 = 2 \times 10^6$.

$$- \frac{4M_p^2}{(m^2 + \phi^2)^3} (m^4 (1 + 2M_p^4) + 2m^2\phi^2 + \phi^4) \Big]. \quad (25)$$

Figure 5 represents the spectral index versus scalar field for $m = 0.2$, $m = 0.5$ and $m = 0.9$. According to WMAP7 [67, 68], WMAP9 [69] and Planck 2015 [70], the value of spectral index lies in the ranges 0.967 ± 0.014 , 0.972 ± 0.013 and 0.968 ± 0.006 .

Using Eqs.(25) and (20), the running of spectral index is calculated as

$$\begin{aligned} \alpha_s = & \frac{32m^4M_p^8}{\phi(m^2 + \phi^2)^{11}} \left(\frac{\beta}{1 + \omega} + v \left(\frac{M_p^4\phi^2}{m^2 + \phi^2} \right)^{(1+\sigma)(1+\omega)} \right)^{\frac{-2(2+\sigma)}{1+\sigma}} \left[\left(\frac{\beta}{1 + \omega} \right)^2 \right. \\ & \times \phi^2 (m^2 + \phi^2)^4 (m^4 (1 + 6M_p^4) + 2m^2\phi^2 + \phi^4) + \left(\frac{M_p^4\phi^2}{m^2 + \phi^2} \right)^{-1+\sigma+\omega+\sigma\omega} \\ & \times (2\phi^{10} + m^{10} (1 + 2M_p^4) (1 + \omega) + m^2\phi^8(9 + \omega) + 4m^4\phi^6(4 + 3M_p^4 \\ & + \omega) + m^8\phi(6\phi + M_p^8(1 + \omega)(3 + 2\omega + 2\sigma(1 + \omega)) + 4\phi(\omega + M_p^4(4 \\ & + \omega))) + m^6\phi^3(-9M_p^8(1 + \omega) + 2\phi(7 + 3\omega + M_p^4(13 + \omega)))) \frac{v\beta M_p^8\phi^4}{1 + \omega} \\ & + M^8v^2\phi^4 \left(\frac{M_p^4\phi^2}{m^2 + \phi^2} \right)^{2(\sigma+\omega+\sigma\omega)} [\phi^{10} + m^{10} (1 + 2M_p^4) (1 + \omega) + m^2\phi^8 \\ & \times (5 + \omega) + 2m^4\phi^6 (5 + 3M_p^4 + 2\omega) + m^6\phi^3(-9M_p^8(1 + \omega) + 2\phi(5 \\ & + 3\omega + M_p^4(7 + \omega))) + m^8\phi[-M_p^8(1 + \omega)(1 + 2\omega) + \phi(5 + 4\omega + 2M_p^4 \\ & \times (5 + 2\omega))]] \Big]. \end{aligned}$$

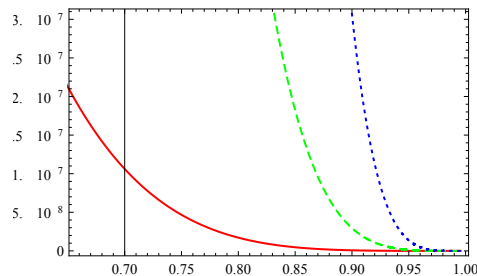


Figure 6: Plot for running of spectral index versus spectral index in weak epoch with $a_0 = 2 \times 10^6$.

The plot of running of spectral index with respect to scalar field is shown in Figure 6. It can be observed that the running of spectral index is compatible with observational data for $m = 0.2$, $m = 0.5$ and $m = 0.9$.

5 Concluding Remarks

The warm MCG inflationary scenario is being investigated with shaft potential for tachyon scalar field. We have discussed this inflationary scenario for both (weak and strong) dissipative regimes in flat FRW universe. We have also examined the results for some of necessary inflationary parameters such as the slow-roll parameters, number of e-folds, scalar-tensor power spectra, spectral indices, tensor-to-scalar ratio and running of scalar spectral index. We have analyzed these parameters for strong epoch as well as weak regime by using the special case of shaft potential. We have restricted constant parameters of the models according to WMAP7 results for examining the physical behavior of $n_s - \phi$, $n_s - R$ and $n_s - \alpha_s$ trajectories in both cases.

We have analyzed the behavior of inflationary parameters according to two dimensionless parameters (a_0, m) where the value of $a_0 = 2 \times 10^6$ remains same for all necessary parameter. All the trajectories are plotted for three different values i.e., $m = 0.2$, $m = 0.5$ and $m = 0.9$. The case for $m = 0.2$ in strong epoch, the plots showed the unsuitable behavior to satisfy the required range of inflationary parameters. However, this value showed the suitable behavior for weak regime. The standard values of parameters are as: the

tensor-to-scalar ratio $r < 0.36, 0.38, 0.11$, the spectral index $n_s = 0.982 \pm 0.020, 0.992 \pm 0.019, 0.9655 \pm 0.0062$ according to WMAP7 [67, 68], WMAP9 [69] and Planck 2015 [70] results respectively. In our case, the tensor-to-scalar ratio versus spectral index is compatible with this observational data (Figure 1 and 4). Also, Figure 3 and 6 clearly showed the compatibility of spectral index for it's running with observational data since observational values of running of spectral index are $\alpha_s = -0.0084 \pm 0.0082, -0.034 \pm 0.026, -0.019 \pm 0.025$ according to Planck 2015 [70], WMAP7 [67, 68] and WMAP9 [69], respectively.

References

- [1] A. Guth , Phys. Rev. D **23**, 347 (1981)
- [2] K. Sato, Mon. Not. Roy. Astron. Soc. **195**, 467 (1981).
- [3] A.D. Linde, Phys. Lett. B **108**, 389 (1982)
- [4] A.D. Linde, Phys. Lett. B **129**, 177 (1983)
- [5] A. Albrecht and P. J. Steinhardt, Phys. Rev. Lett. **48**,1220 (1982)
- [6] A. D. Linde, Phys. Lett. B **129** (1983) 177.
- [7] V.F. Mukhanov and G.V. Chibisov , JETP Letters **33**, 532(1981)
- [8] S. W. Hawking,Phys. Lett. B **115**, 295 (1982)
- [9] A. Guth and S.-Y. Pi, Phys. Rev. Lett. **49**, 1110 (1982)
- [10] A. A. Starobinsky, Phys. Lett. B **117**, 175 (1982)
- [11] J.M. Bardeen, P.J. Steinhardt and M.S. Turner, Phys. Rev.D **28**, 679 (1983).
- [12] D. Larson *et al.*, Astrophys. J. Suppl. **192**, 16 (2011).
- [13] C. L. Bennett *et al.*, Astrophys. J. Suppl. **192**, 17 (2011)
- [14] N. Jarosik *et al.*, Astrophys. J. Suppl. **192**, 14 (2011)

- [15] G. Hinshaw *et al.* [WMAP Collaboration], *Astrophys. J. Suppl.* **208**, 19 (2013)
- [16] P. A. R. Ade *et al.* [Planck Collaboration], *Astron. Astrophys.* **571**, A16 (2014)
- [17] P. A. R. Ade *et al.* [Planck Collaboration], *Astron. Astrophys.* **571**, A22 (2014).
- [18] P. A. R. Ade *et al.* [Planck Collaboration], *Astron. Astrophys.* **594**, A13 (2016).
- [19] P. A. R. Ade *et al.* [Planck Collaboration], *Astron. Astrophys.* **594**, A20 (2016).
- [20] L. Kofman, A. D. Linde and A. A. Starobinsky, *Phys. Rev. Lett.* **73**, 3195 (1994)
- [21] L. Kofman, A. D. Linde and A. A. Starobinsky, *Phys. Rev. D* **56**, 3258 (1997).
- [22] M. A. Amin, M. P. Hertzberg, D. I. Kaiser and J. Karouby, *Int. J. Mod. Phys. D* **24**, 1530003 (2014)
- [23] I.G. Moss, *Phys.Lett.B* **154**, 120 (1985). A. Berera, *Phys. Rev. Lett.* **75**, 3218 (1995).
- [24] A. Berera, *Phys. Rev. D* **55**, 3346 (1997)
- [25] Y. Zhang, *JCAP* **0903**, 023 (2009).
- [26] M. Bastero-Gil, A. Berera, R. O. Ramos and J. G. Rosa, *JCAP* **1301**, 016 (2013).
- [27] A.D. Linde: *Phys. Lett. B* **129**(1983)177.
- [28] R. Herrera: *Phys. Rev. D* **81**(2010)123511.
- [29] S. Del Campo and R. Herrera: *Phys. Lett. B* **660**(2008)282.
- [30] M.R. Setare and V., Kamali: *JCAP* **08**(2012).
- [31] M.R. Setare and V., Kamali: *Phys. Rev. D* **87**(2013)083524.

- [32] Bastero-Gil, M., Berera, A., Ramos, R.O., Rosa, J.G.: JCAP **1301**(2013)016.
- [33] M. Bastero-Gil, A. Berera, R.O. Ramos, J.G. Rosa: JCAP **1410**(2014)10053.
- [34] R. Herrera, M. Olivares and N. Videla: Eur. Phys. J. C **73**(2013)2295.
- [35] Panotopoulos, G. and Videla, N.: Eur. Phys. J. C **75**(2015)525.
- [36] Jawad, A., Ilyas, A. and Rani, S.: Int. J. Mod. Phys. D **26**(2017)1750031; Astroparticle Phys. **81**(2016)61; Jawad, A., Rani, S. and Mohsaneen, S.: Eur. Phys. J. Plus **131**(2016)234; Astrophys. Space Sci. **361**(2016)158; Jawad, A., Butt, S. and Rani, S.: Astrophys. Space Sci. **361**(2016)258; Eur. Phys. J. C **76**(2016)274.
- [37] Bamba, K. and Odintsov, S.D.: Eur. Phys. J. C **76**(2016)18; Bamba, K., Odintsov, S.D. and Tretyakov, P.V.: Eur. Phys. J. C **75**(2015)344; Sanchez, J. C. B., Bastero-Gil, M. Berera, A. and Dimopoulos, K.: Phys. Rev. D **77**(2008)123527; Herrera, R.: Phys. Rev. D **81**(2010)123511; Herrera, R. and San Martin, E.: Eur. Phys. J. C **71**(2011)1701; Herrera, R., Olivares, M. and Videla, N.: Eur. Phys. J. C **73**(2013)2295; Phys. Rev. D **88**(2013)063535.
- [38] K. Dimopoulos: Phys. Lett. B **735**(2014)75.
- [39] P. J. E. Peebles and B. Ratra, Rev. Mod. Phys. **75**, 559 (2003).
- [40] B. Ratra and P. J. E. Peebles, Phys.Rev. D **37**, 3406 (1988).
- [41] R. R. Caldwell, R. Dave and P. J. Steinhardt, Phys. Rev. Lett. **80**, 1582 (1998).
- [42] M. Sami and T. Padmanabhan, Phys. Rev. D **67**, 083509 (2003).
- [43] C. Armendariz-Picon, V. Mukhanov and P. J. Steinhardt, Phys. Rev. D **63**, 103510 (2001) .
- [44] T. Chiba, Phys. Rev. D **66**, 063514 (2002) .
- [45] R. J. Scherrer, Phys. Rev. Lett. **93**, 011301 (2004).

- [46] A. Sen, J. High Energy Phys. **04**, 048 (2002) .
- [47] A. Sen, J. High Energy Phys. **07**, 065 (2002) .
- [48] G.W. Gibbons, Phys. Lett. B **537**, 1 (2002) .
- [49] R. R. Caldwell, Phys. Lett. B **545**, 23 (2002) .
- [50] E. Elizade, S. Nojiri and S. Odintsov, Phys. Rev. D **70**, 043539 (2004) .
- [51] J. M. Cline, S. Jeon and G. D. Moore, Phys. Rev. D **70**, 043543 (2004).
- [52] A. Kamenshchik, U. Moschella and V. Pasquier, Phys. Lett. B **511**, 265 (2001).
- [53] M. Li, Phys. Lett. B **603**, 1 (2004).
- [54] M.C. Bento, O. Bertolami and A.A. Sen, Phys.Rev. D **70**, 083519 (2004).
- [55] Bento, M. C., Bertolami, O., and Sen, A. A., Phys. Lett. **B 575**, 172 (2003).
- [56] M. Makler, S. Quinet de Oliveira and I. Waga, Phys. Lett. B **555**, 1 (2003)
- [57] L. Amendola, F. Finelli, C. Burigana and D. Carturan, JCAP **0307**, 005 (2003).
- [58] H. B. Benaoum, hep-th/0205140.
- [59] J. Lu, L. Xu, J. Li, B. Chang, Y. Gui and H. Liu, Phys. Lett. B **662**, 87 (2008).
- [60] U. Debnath, A. Banerjee and S. Chakraborty, Class. Quant. Grav. **21**, 5609 (2004).
- [61] S. Silva e Costa, M. Ujevic and A. Ferreira dos Santos, Gen. Rel. Grav. **40**, 1683 (2008).
- [62] L. Amendola and S. Tsujikawa: Cambridge Univ. Press, Cambridge, UK, (2010)172.
- [63] S.D. Campo, R. Herrera, D. Pavon and J.R. Villanueva: JCAP **002**(2010)1008.

- [64] Y. Zhang: JCAP **023**(2009)0903.
- [65] A. R. Liddle and D. H. Lyth: Phys. Lett. B **291**(1992)391.
- [66] M. Czerny, T. Kobayashi and F. Takahashi: Phys. Lett. B **735**(2014)176.
- [67] E. Komatsu et al.: Astrophys. J. Suppl. **192**(2011)18.
- [68] D. Larson et al.: Astrophys. J. Suppl. **192**(2011)16.
- [69] G. Hinshaw et al.: Astrophys. J. Suppl. **208**(2013)19.
- [70] P. A. R. Ade et al.: arXiv:1502.01589.

